

# Dual functions of ARP101 in targeting membrane type-1 matrix metalloproteinase: Impact on U87 glioblastoma cell invasion and autophagy signaling

Michel Desjarlais | Borhane Annabi 

Laboratoire d'Oncologie  
Moléculaire, Département de  
Chimie, Centre de recherche  
BIOMED, Université du Québec à  
Montréal, Montréal, Quebec, Canada

## Correspondence

Borhane Annabi, Laboratoire d'Oncologie  
Moléculaire, Université du Québec à  
Montréal, Montréal, QC, Canada.  
Email: annabi.borhane@uqam.ca

## Funding information

Institutional Research Chair in Cancer  
Prevention and Treatment

## Abstract

Membrane type-1 matrix metalloproteinase (MT1-MMP) possesses both extracellular proteolytic and intracellular signal-transducing functions in tumorigenesis. An imbalance in MT1-MMP expression and/or function triggers a metastatic, invasive, and therapy resistance phenotype. MT1-MMP is involved in extracellular matrix (ECM) proteolysis, activation of latent MMPs, as well as in autophagy signaling in human hepatoma and glioblastoma cells. A low autophagy index in tumorigenesis has been inferred by recent studies where autophagic capacity was decreased during tumor progression. Here, we establish ARP101 as a dual-function small-molecule inhibitor against MT1-MMP ECM hydrolysis and autophagy signal-transducing functions in a model of grade IV glioblastoma cells. ARP101 inhibited concanavalin-A-mediated proMMP-2 activation into MMP-2, as well as MT1-MMP auto-proteolytic processing. When overexpressing recombinant Wt MT1-MMP, ARP101 inhibited proMMP-2 activation and triggered the formation of MT1-MMP oligomers that required trafficking to the plasma membrane. ARP101 further induced cell autophagy as reflected by increased formation of acidic vacuole organelles, LC3 puncta, and autophagy-related protein ATG9 transcription. These were all significantly reversed upon siRNA-mediated gene silencing of MT1-MMP. ARP101 can thus concomitantly inhibit MT1-MMP extracellular catalytic function and exploit its intracellular transducing signal function to trigger autophagy-mediated cell death in U87 glioblastoma cancer cells.

## KEYWORDS

ARP101, autophagy, concanavalin-A, glioblastoma, MT1-MMP processing

## 1 | INTRODUCTION

One of the compelling reasons of brain cancer therapy failure relates to the adaptive metabolic mechanisms that lead to their resistance phenotype, which makes it difficult

to foresee their response to any treatment.<sup>[1,2]</sup> Among the therapy resistance mechanisms that regulate cancer cell death/survival balance, the fundamental importance of autophagy in the development and progression of cancer has recently been highlighted.<sup>[3-5]</sup> In grade IV glioblastoma, the most fatal tumor of the central nervous system,<sup>[6]</sup> mounting evidence suggests that autophagy processes are tightly associated with tumorigenesis.<sup>[7,8]</sup> Although high-grade gliomas are characterized with reduced expression of

**Abbreviations:** ATG, autophagy-related proteins; ConA, concanavalin-A; ECM, extracellular matrix; MT1-MMP, membrane type-1 matrix metalloproteinase.

autophagy-related proteins (ATG) when compared to low-grade gliomas,<sup>[9,10]</sup> it is still unclear whether dysregulation of autophagy in advanced brain cancer would promote survival or death upon various therapeutic settings.

Given dysregulation of autophagy is closely linked to therapy resistance in cancer, targeting autophagy is currently being exploited as a novel therapeutic strategy for clinical utility. Recently, the alkylating drug temozolomide, which is routinely used in brain tumor patients, was found to induce apoptosis, autophagy, and unfolded protein response,<sup>[11]</sup> but has been disappointing against the highly invasive and resistant nature of glioblastoma.<sup>[12]</sup> Other molecules such as FTY720, a synthetic compound which has been approved by the US Food and Drug Administration to treat relapsed multiple sclerosis,<sup>[13]</sup> was also found to induce autophagy-related apoptosis and necroptosis and to inhibit invasion and migration in human glioblastoma cells.<sup>[14,15]</sup> FTY720 has recently been also found to sensitize glioblastoma cells to temozolomide.<sup>[16]</sup>

Design of small-molecule autophagy modulators therefore appears to be a promising druggable strategy.<sup>[17]</sup> Among these, ARP101, originally characterized for its inhibitory property against matrix metalloproteinase 2 (MMP-2) catalytic functions, was found to also trigger autophagy in cells of mouse embryo fibroblasts.<sup>[18]</sup> Such functional dual targeting properties of ARP101 make this molecule a privileged drug in future selective targeting modalities. Among specific brain cancer biomarkers characterized by both MMP catalytic functions and autophagy inducing properties, membrane type-1 (MT1) MMP, a key membrane bound MMP involved in tumor invasion, was classically ascribed an active role in extracellular matrix (ECM) degradation<sup>[19–21]</sup> and, more recently, signal-transducing functions leading to angiogenesis,<sup>[22]</sup> autophagy,<sup>[23,24]</sup> inflammation,<sup>[25,26]</sup> immune response,<sup>[27]</sup> and cell death processes.<sup>[28,29]</sup> Since autophagy plays a dual role in oncogenesis, where low autophagy promotes cancer cell survival in response to constant stress,<sup>[30]</sup> but when strongly induced can also trigger cell death of type 3 and lead to complete cellular self-digestion,<sup>[31]</sup> any pharmacological approach that would disrupt the homeostatic balance of autophagy may therefore be exploited within antitumor modalities.

The oncogenic contribution of MT1-MMP in tumor invasion is not only controlled through the extent of its expression levels, but also through its auto-regulatory processing and oligomerization states.<sup>[32–34]</sup> Indeed, MT1-MMP can regulate itself by auto-proteolytic cleavage that generates an inactive 43 kD form,<sup>[35]</sup> whereas dimerization of MT1-MMP is rather believed to facilitate the activation of proMMP-2.<sup>[34]</sup> While the homo-oligomer formation of MT1-MMP has recently been revealed in several studies, its biological significance remains misunderstood.<sup>[36,37]</sup> In the current study, we

investigated the dual pharmacological actions of ARP101 on MT1-MMP-mediated proMMP-2 activation as well as on the involvement of MT1-MMP in signaling autophagy in an established grade IV glioblastoma cell model.

## 2 | METHODS AND MATERIALS

### 2.1 | Materials

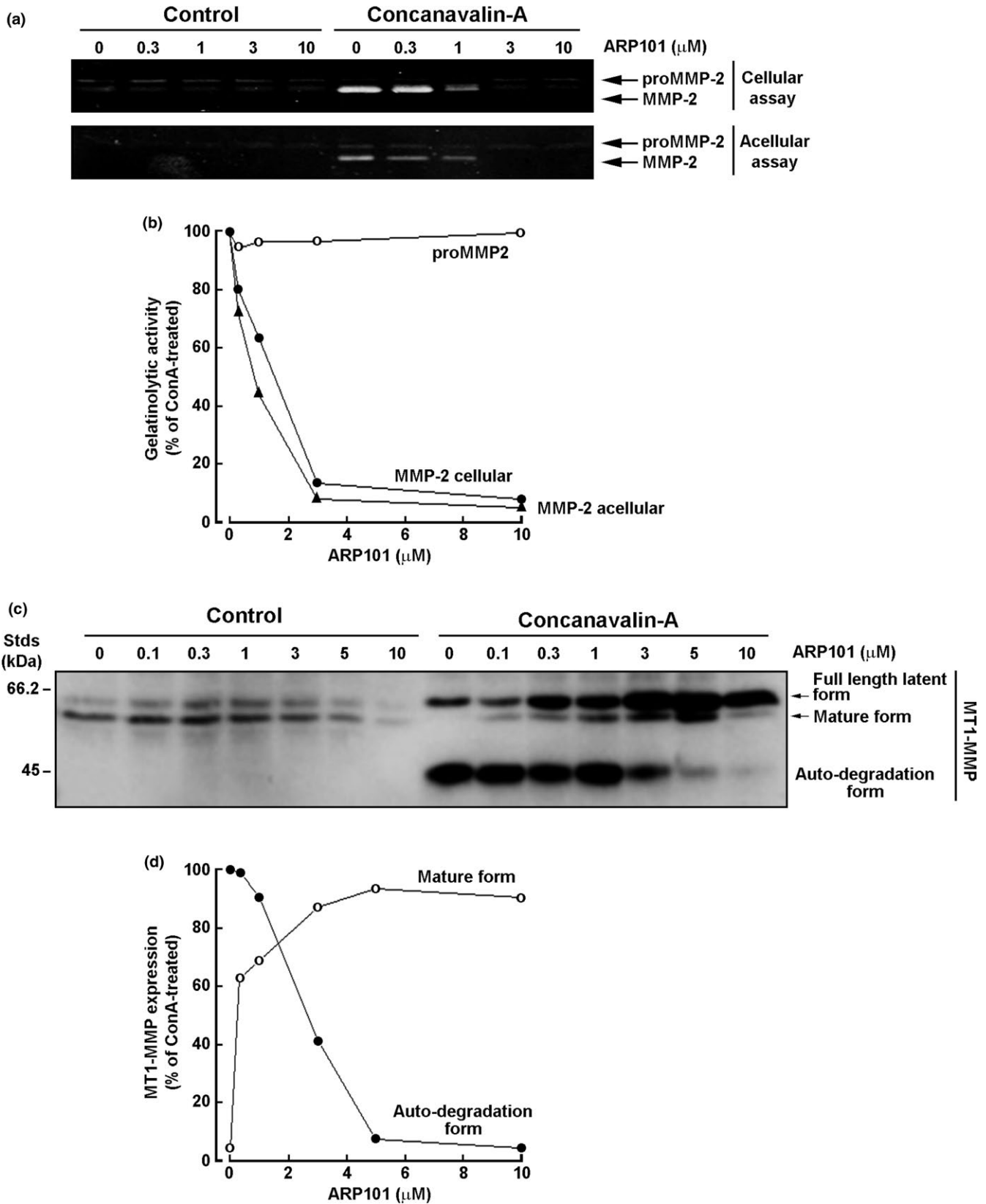
Sodium dodecyl sulfate (SDS), ARP101, and bovine serum albumin (BSA) were purchased from Sigma (Oakville, ON). Electrophoresis reagents were from Bio-Rad (Mississauga, ON). The enhanced chemiluminescence (ECL) reagents were from Amersham Pharmacia Biotech (Baie d'Urfé, QC). Micro bicinchoninic acid protein assay reagents were from Pierce (Rockford, IL). The polyclonal antibody against the MT1-MMP hinge domain was from Chemicon (Temecula, CA). The monoclonal antibody against glyceraldehyde 3-phosphate dehydrogenase (GAPDH) was from Advanced Immunochemical Inc. (Long Beach, CA, USA). Horseradish peroxidase-conjugated donkey anti-rabbit and anti-mouse IgG secondary antibodies were from Jackson ImmunoResearch Laboratories (West Grove, PA, USA).

### 2.2 | Cell culture

Human U87 glioblastoma cells were purchased from American Type Culture Collection (ATCC; Manassas, VA). Serum starvation is classically performed by culturing the cells in Eagle's minimal essential medium (EMEM; Gibco BRL) and 100 units/ml penicillin/streptomycin, and from which the 10% inactivated fetal bovine serum (Hyclone Laboratories, Logan, UT) is removed.

### 2.3 | Immunoblotting procedures

Human U87 glioblastoma cells were lysed, and proteins were separated by SDS-polyacrylamide gel electrophoresis (PAGE). In order to detect MT1-MMP oligomer formation, samples were subjected to SDS-PAGE gels in non-reducing conditions. After electrophoresis, proteins (30 µg) were electrotransferred to polyvinylidene difluoride membranes, which were then blocked for 1 hr at room temperature with 5% nonfat dry milk in Tris-buffered saline (150 mM NaCl, 20 mM Tris-HCl, pH 7.5) containing 0.3% Tween-20 (TBST; Bioshop, TWN510-500). Membranes were further washed in TBST and incubated with the anti-MT1-MMP or anti-GAPDH primary antibodies (1/1,000 dilution) in TBST containing 3% BSA and 0.1% sodium azide (Sigma-Aldrich Canada, S2002), followed by an 1-hr incubation with horseradish peroxidase-conjugated donkey anti-rabbit IgG at 1/2,500 dilutions in



TBST containing 5% nonfat dry milk. Immunoreactive material was visualized by enhanced chemiluminescence (Amersham Pharmacia Biotech, RPN3004). MT1-MMP immunoreactivity of both the latent proMT1-MMP

(63 kDa) and active MT1-MMP (60 kDa) forms was collectively defined as detection of “mature form” in contrast to its inactive MT1-MMP (43 kDa) form defined as “proteolytic form” where indicated.

**FIGURE 1** ARP101 inhibits concanavalin-A-induced proMMP-2 activation and membrane type-1 matrix metalloproteinase (MT1 MMP) proteolytic processing. Serum-starved U87 glioblastoma cells were treated with or without 30  $\mu\text{g/ml}$  concanavalin-A for 24 hr in the presence of various concentrations (0–10  $\mu\text{M}$ ) of ARP101. (a) Conditioned media were harvested in order to assess the extent of proMMP-2 activation by gelatin zymography as described in the section 2 in a cellular assay (i.e. cells were treated with ARP101, and then, conditioned media were harvested) or in an acellular assay (i.e. conditioned media from untreated cells were harvested then subjected to treatment with ARP101). (b) A representative scanning densitometry analysis of gelatinolytic activity is presented for cellular and acellular treatments. (c) Protein expression of full-length latent (63 kDa), mature (60 kDa), and auto-degradation (43 kDa) forms of MT1-MMP was assessed by Western blotting and immunodetection performed as described in the section 2. (d) The level of expression of the mature and auto-degradation MT1-MMP forms was quantified by scanning densitometry

## 2.4 | Gelatin zymography

Gelatin zymography was used to assess the extracellular levels of secreted proMMP-2 and MMP-2 activities. Briefly, an aliquot (20  $\mu\text{l}$ ) of the culture medium was subjected to SDS-PAGE in a gel containing 0.1 mg/ml gelatin (Sigma-Aldrich Canada, G2625). The gels were then incubated in 2.5% Triton X-100 (Bioshop, TRX506.500) and rinsed in nanopure distilled water. Gels were further incubated at 37°C for 20 hr in 20 mM NaCl, 5 mM  $\text{CaCl}_2$ , 0.02% Brij-35, 50 mM Tris-HCl buffer, pH 7.6 and then stained with 0.1% Coomassie Brilliant blue R-250 (Bioshop, CBB250) and destained in 10% acetic acid, 30% methanol in water. Gelatinolytic activity was detected as unstained bands on a blue background.

## 2.5 | Total RNA isolation, cDNA synthesis, and real-time quantitative PCR

Total RNA was extracted from U87 glioblastoma cell monolayers using TRIzol reagent (Life Technologies, Gaithersburg, MD). For cDNA synthesis, 1  $\mu\text{g}$  of total RNA was reverse-transcribed into cDNA using a high capacity cDNA reverse transcription kit (Applied Biosystems, Foster City, CA). cDNA was stored at  $-80^\circ\text{C}$  prior to PCR. Gene expression was quantified by real-time quantitative PCR using iQ SYBR Green Supermix (Bio-Rad, Hercules, CA). DNA amplification was carried out using an Icyler iQ5 (Bio-Rad, Hercules, CA), and product detection was performed by measuring binding of the fluorescent dye SYBR Green I to double-stranded DNA. The following primer sets were provided by QIAGEN (Valencia, CA): MT1-MMP (HS\_MMP14\_1\_SG, QT00001533), ATG3 (Hs\_ATG3\_1\_SG, QT00069769), ATG5 (Hs\_ATG5\_1\_SG, QT00073325), ATG9 (Hs\_ATG9B\_2\_SG, QT01159956), ATG12 (Hs\_ATG12\_1\_SG, QT00035854), ATG16L1 (Hs\_ATG16L1\_1\_SG, QT00085442), GAPDH (Hs\_GAPDH\_2\_SG, QT01192646), and  $\beta$ -actin (Hs\_Actb\_2\_SG, QT01680476). The relative quantities of target gene mRNA against an internal control  $\beta$ -actin RNA were measured by following a  $\Delta C_T$  method employing an amplification plot (fluorescence signal vs. cycle number). The difference ( $\Delta C_T$ ) between the mean values in the triplicate samples of target gene and those of

$\beta$ -actin RNA were calculated by CFX manager Software version 2.1 (Bio-Rad), and the relative quantified value (RQV) was expressed as  $2^{-\Delta C_T}$ .

## 2.6 | Transfection method of cDNA plasmids and RNA interference

U87 glioblastoma cells were transiently transfected with plasmids or siRNA sequences using Lipofectamine-2000 transfection reagent (Thermo Fisher Scientific, Waltham, MA). cDNA plasmids used included Wt-MT1-MMP<sup>[24]</sup> or pEGFP-LC3 (generously provided by Dr Patrick Labonté, INRS-IAF, Qc). Gene silencing was performed using 20 nM siRNA against MT1-MMP (HS\_Mmp14\_6 HP siRNA, S103648841) or scrambled sequences (AllStar Negative Control siRNA, 1027281). The above small interfering RNA and mismatch siRNA were all synthesized by QIAGEN and annealed to form duplexes.

## 2.7 | Detection of acidic vesicular organelles and of LC3 puncta

Mock or transfected U87 glioblastoma cells were serum-starved and then treated with or without 10  $\mu\text{M}$  ARP101. acridine orange (0.5  $\mu\text{g/ml}$ ; Sigma-Aldrich, ON) was added to each well for chromatin and acidic vacuoles staining, and then, cells were incubated for 10 min at 37°C in the dark. By intercalation between the lower and upper purine and pyrimidine DNA rings of  $\sim$  each third nucleotide base pair, acridine orange produces a green emission peak of the monomeric dye form (max:  $\sim$ 530 nm), while the acridine orange dimers produce a red emission peak (max: 640 nm) within acidic vacuoles. Both can be excited by an argon laser (488 nm) using a confocal microscope. For LC3 punctate formation, transient cell transfection was performed with pEGFP-LC3,<sup>[38]</sup> GFP fluorescence was examined by microscopy, and punctate quantified using image J software.

## 2.8 | Statistical data analysis

Data are representative of three or more independent experiments. Statistical significance was assessed using Student's unpaired *t* test probability values of  $<0.05$  were considered

significant, and an asterisk identifies such significance in the figures.

### 3 | RESULTS

#### 3.1 | ARP101 inhibits concanavalin-A-induced proMMP-2 activation and MT1-MMP proteolytic processing

We first wished to validate whether inhibition of the MMP hydrolytic activity by ARP101 also targeted MT1-MMP auto-proteolytic processing activity. Concanavalin-A (ConA), a lectin classically known to trigger MT1-MMP-mediated proMMP-2 activation and MT1-MMP auto-proteolytic activity, was used.<sup>[39]</sup> We decided to perform a cellular and an acellular evaluation of ARP101. First for the cellular assay, serum-starved U87 glioblastoma cells were treated with or without 30  $\mu\text{g/ml}$  ConA in the presence of increasing concentrations of ARP101. Conditioned media were harvested in order to assess the extent of proMMP-2 activation by gelatin zymography (Figure 1a, upper panel). Whereas proMMP-2 levels remained unaltered (Figure 1b, open circle), we observed that ARP101 dose-dependently inhibited proMMP-2 activation into MMP-2 (Figure 1b, closed circle). ARP101 was also assessed for its capacity to directly inhibit MMP-2 in an acellular tube assay, which consisted of conditioned media harvested from ConA-treated cells (Figure 1a, lower panel). We observed that ARP101 dose-dependently inhibited MMP-2 gelatinolytic activity, which confirms ARP101 capacity to directly interact with the MMP-2 catalytic site (Figure 1b, closed triangle). Cell lysates were isolated from control or ConA-treated conditions and immunoblotting performed to assess the extent of ConA-mediated MT1-MMP auto-proteolytic processing (Figure 1c). We have defined the MT1-MMP auto-degradation form as “the form which is auto-catalytically processed from its 55- to 60-kDa form into its inactive 43-kDa form.” We found that ARP101 dose-dependently inhibited MT1-MMP auto-proteolytic processing as shown by the disappearance of its auto-degradation 43 kDa form triggered upon ConA treatment and the accumulation of MT1-MMP mature form (Figure 1d). These observations suggest that ARP101 possesses affinity toward the catalytic sites of both MMP-2 and MT1-MMP. Furthermore, the targeting of MT1-MMP “activation process” by ARP101 itself (i.e. in the absence of ConA, Figure 1c left conditions) is strongly supportive of a possible involvement of a Furin-mediated process which inhibition by ARP101 is effectively possible. Whereas in ConA treatment (Figure 1c right conditions), two processes are combined in the regulation of MMP14, namely, Furin-mediated maturation as well as MT1-MMP autocatalytic processing, which could be targeted by ARP101.

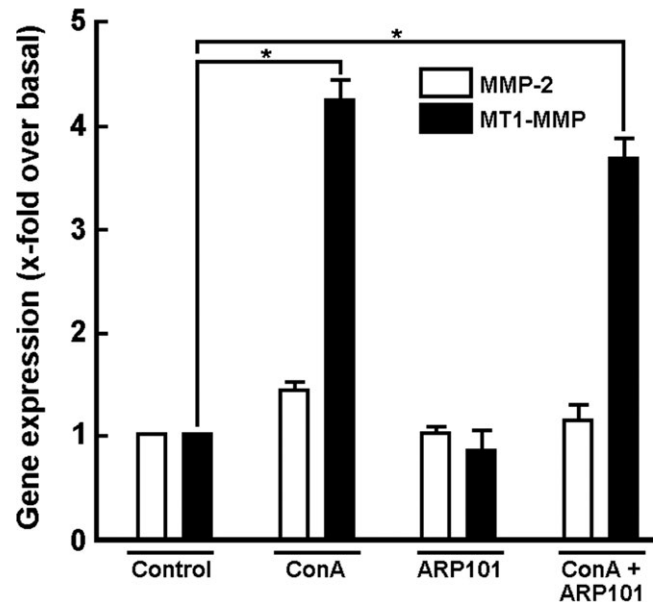


**FIGURE 2** ARP101 does not alter the transcriptional control of matrix metalloproteinase 2 (MMP-2) and membrane type-1 (MT1)-MMP. MMP-2 and MT1-MMP gene expression was assessed in U87 glioblastoma cells that were treated with or without 10  $\mu\text{M}$  ARP101 in the presence or absence of 30  $\mu\text{g/ml}$  concanavalin-A (ConA) for 24 hr. Total RNA was isolated, cDNA synthesized and qPCR performed as described in the section 2

#### 3.2 | ARP101 does not alter MMP-2 and MT1-MMP gene expression

We next explored whether ARP101 treatment may also affect transcriptional regulation of MMP-2 or MT1-MMP. U87 glioblastoma cells were treated with or without 30  $\mu\text{g/ml}$  ConA in the presence or absence of 10  $\mu\text{M}$  ARP101. Total RNA was isolated as described in the section 2, and MT1-MMP and MMP-2 gene expressions were assessed using RT-qPCR. We found that MMP-2 gene expression was not altered upon any of the cell treatments performed (Figure 2, white bars). This was also the case for MT1-MMP gene expression, where even the ConA-induced MT1-MMP levels were not affected by ARP101 (Figure 2, black bars). These results suggest that ARP101 specifically affects MT1-MMP extracellular hydrolytic functions through a post-translational mechanism.

#### 3.3 | ARP101 triggers recombinant MT1-MMP oligomerization that correlates with the inhibition of MT1-MMP auto-proteolytic processing

To further investigate the inhibitory function of ARP101 on MT1-MMP auto-proteolytic function, we transiently transfected U87 glioblastoma cells with a cDNA plasmid encoding Wt MT1-MMP as described in the section 2. We next treated serum-starved cells with increasing concentrations of ARP101,

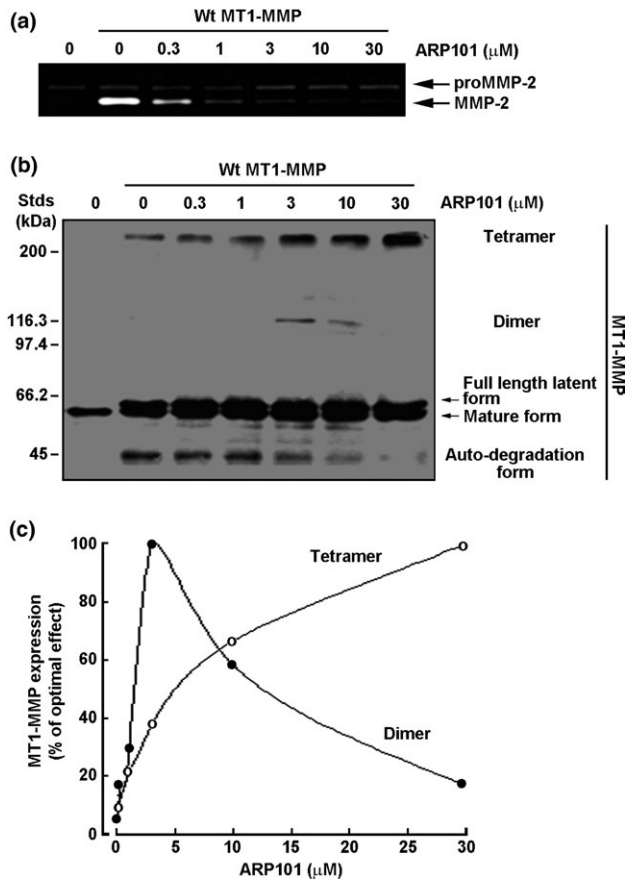


**FIGURE 3** ARP101 triggers recombinant membrane type-1 matrix metalloproteinase (MT1-MMP) oligomerization that correlates with the inhibition of proMMP-2 activation and of MT1-MMP auto-proteolytic processing. U87 glioblastoma cells were transiently transfected with a plasmid cDNA encoding recombinant MT1-MMP (Wt MT1-MMP) as described in the section 2. Serum-starved cells were then treated with increasing concentrations of ARP101. (a) Conditioned media were isolated to assess the extent of proMMP-2 activation by gelatin zymography. (b) Protein expression of the tetramer (240 kDa), dimer (120 kDa), full-length latent (63 kDa), mature (60 kDa), and auto-degradation (43 kDa) MT1-MMP forms was assessed by immunoblotting and (c) quantified by scanning densitometry

isolated the conditioned media to assess the extent of proMMP-2 activation, and lysed the cells for MT1-MMP immunoblotting. Overexpression of recombinant MT1-MMP effectively triggered proMMP-2 activation into MMP-2, which was inhibited by increasing ARP101 concentrations (Figure 3a). When recombinant MT1-MMP protein expression was assessed, we found again that ARP101 inhibited the auto-proteolytic activity as the inactive 43 kDa auto-degradation form of MT1-MMP decreased with increasing ARP101 concentrations (Figure 3b). Interestingly, MT1-MMP dimers (130 kDa) as well as tetramers (240 kDa) were observed. Tetramers were increasingly expressed, whereas transient dimerization was observed peaking at 3  $\mu\text{M}$  ARP101 (Figure 3c). Overall, this suggests that ARP101 capacity to inhibit

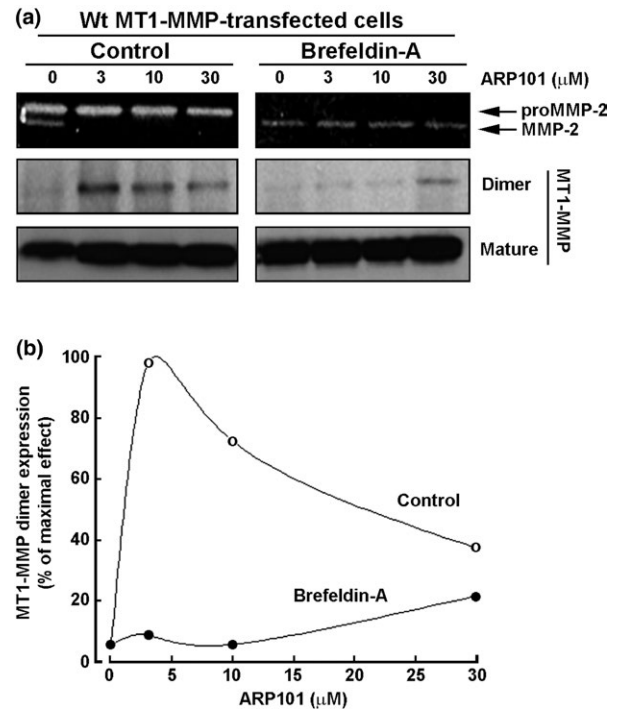


**FIGURE 4** ARP101-mediated effects on membrane type-1 matrix metalloproteinase (MT1-MMP) oligomerization and proteolytic processing requires MT1-MMP cell surface location. U87 glioblastoma cells were transiently transfected with a plasmid cDNA encoding a full-length MT1-MMP (Wt MT1-MMP) as described in the section 2. Serum-starved cells were then treated with increasing concentrations of ARP101 in the presence or not of 1  $\mu\text{M}$  Brefeldin-A. (a) Conditioned media were harvested in order to assess the extent of proMMP-2 activation by gelatin zymography (upper panel), whereas cell lysates were used to assess the extent of MT1-MMP mature and dimer forms by Western blotting (middle and lower panels), and (b) quantified by scanning densitometry

MT1-MMP auto-proteolytic activity promoted cell surface oligomerization which correlated with decreased capacity to activate latent proMMP-2. The functional composition of the oligomers as observed by Western blotting remains unknown. Whether these forms represent combinations of inactive MT1-MMP proteolytic forms to active MT1-MMP also remains to be determined.

### 3.4 | ARP101-mediated effects on MT1-MMP oligomerization and proteolytic processing requires its cell surface location

In order to better investigate the subcellular compartmentation process involved in ARP101-mediated MT1-MMP oligomerization, we used Brefeldin-A, a vesicular trafficking inhibitor.<sup>[40]</sup> U87 glioblastoma cells were transiently transfected with a cDNA plasmid encoding Wt-MT1-MMP, then were treated with increasing ARP101 concentrations. Conditioned media and cell lysates were harvested to perform gelatin zymography (Figure 4a, upper panel)

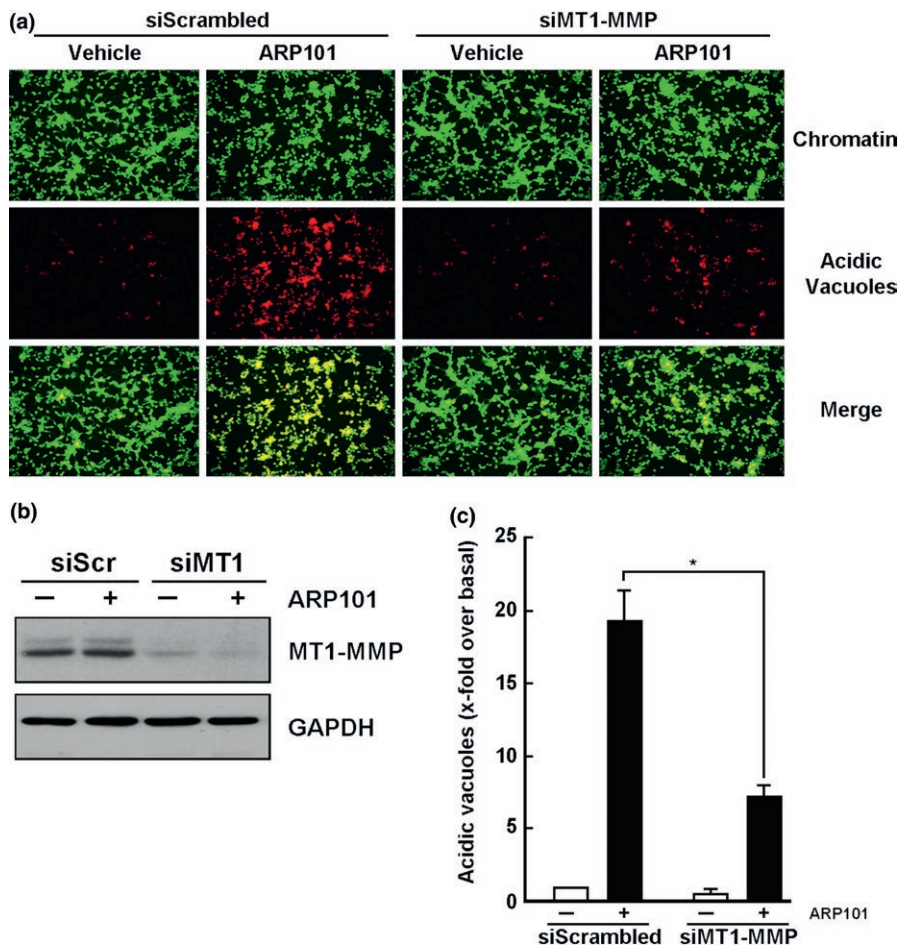


**FIGURE 5** ARP101 triggers the formation of intracellular acidic vacuoles and requires membrane type-1 matrix metalloproteinase (MT1-MMP) transducing functions. U87 glioblastoma cells were transiently transfected with a control siRNA (siScrambled) or a siRNA directed against MT1-MMP (siMT1-MMP) as described in the section 2. Cells were then serum-starved and treated with 10  $\mu$ M ARP101 for 24 hr. (a) Cells were stained with acridine orange as described in the section 2. Acidic vacuole formation (red), chromatin (green), and merged pictures (yellow) were visualized, (b) MT1-MMP and GAPDH protein expression levels were assessed by immunoblotting. (c) Cell fluorescence was used to quantify acidic vacuoles formation using confocal microscopy as described in the section 2. Representative pictures are shown and a mean fluorescence measured from four independent experiments for each condition [Colour figure can be viewed at [wileyonlinelibrary.com](http://wileyonlinelibrary.com)]

and immunoblotting (Figure 4a, middle and lower panels), respectively. We found that inhibiting MT1-MMP trafficking to the cell surface inhibited MT1-MMP-mediated proMMP-2 activation and disabled ARP101 capacity to trigger MT1-MMP dimerization (Figure 4b). This suggests that ARP-mediated MT1-MMP oligomerization is performed at the plasma membrane.

### 3.5 | ARP101 requires MT1-MMP transducing functions to trigger autophagy through the formation of intracellular acidic vacuoles and LC3 puncta

ARP101 has also been documented as a potent inducer of autophagy, although the exact mechanism involved remains poorly understood. Given the above-described ARP101 capacity to interact with MT1-MMP extracellular functions, we next assessed the involvement of MT1-MMP-mediated intracellular signaling of autophagy.<sup>[23,38]</sup> Serum-starved U87 glioblastoma cells were transiently transfected with a control siRNA (siScrambled) or a siRNA directed against MT1-MMP (siMT1-MMP), then treated with or without 10  $\mu$ M ARP101 for 24 hr. Finally, cells were stained for chromatin content (Figure 5a, upper panel, green) or acidic vacuoles formation (Figure 5a, middle panel, red). While none of the conditions tested altered

chromatin content, ARP101 clearly triggered acidic vacuoles formation associated with autophagic cells (Figure 5a, bottom panel, yellow), which was significantly reversed upon MT1-MMP repression, as confirmed by Western blot (Figure 5b) and fluorescence analysis (Figure 5c). In order to confirm involvement of MT1-MMP in ARP101-mediated autophagy, we next transiently co-transfected cells with siMT1-MMP and a plasmid cDNA encoding GFP-LC3, a classical approach used to monitor the formation of the autophagosome as observable by the formation of puncta.<sup>[41]</sup> Serum-starved cells were then treated with 10  $\mu$ M ARP101. Only green fluorescent cells were analyzed, and two pictures per condition are shown (Figure 6a). We observed that ARP101 effectively induced LC3 punctates, whereas the number of punctates was attenuated upon MT1-MMP repression (Figure 6b).

### 3.6 | ARP101 induces ATG9 autophagy biomarker gene expression and requires MT1-MMP transducing functions

As a final approach to document the involvement of autophagy in ARP101-mediated events, we screened autophagy biomarkers ATG3, ATG5, ATG9, ATG12, and ATG16 gene expression levels and their potential modulation upon MT1-MMP repression. Cells were treated with or without

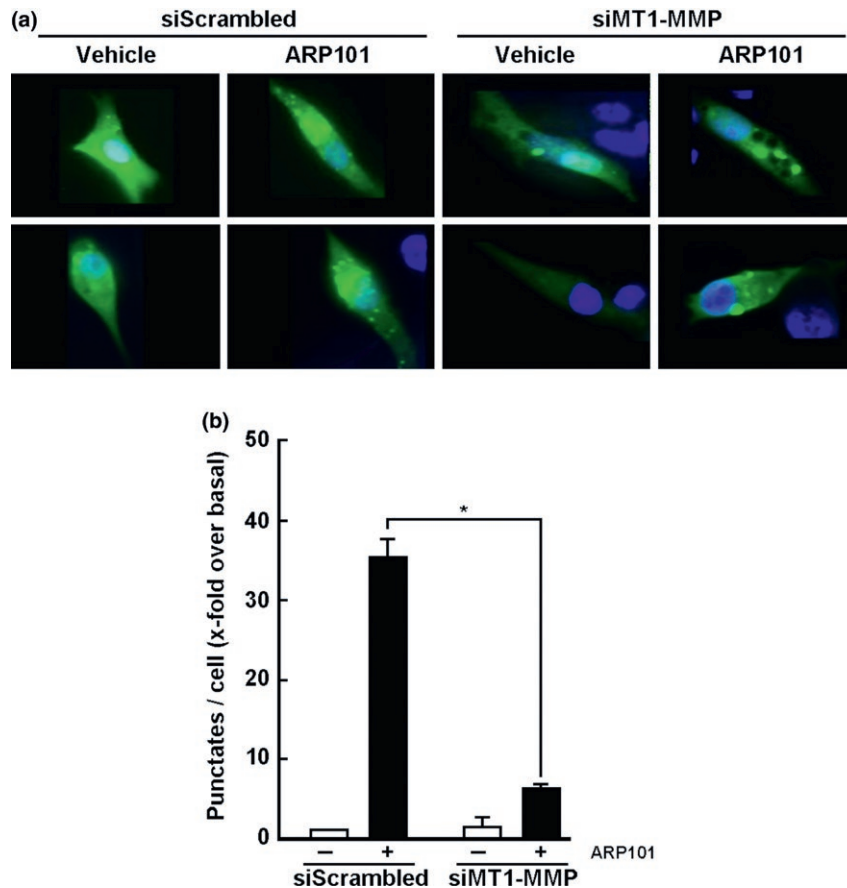


**FIGURE 6** ARP101 triggers autophagy LC3 punctates and requires membrane type-1 matrix metalloproteinase (MT1-MMP) intracellular transducing functions. U87 glioblastoma cells were transiently co-transfected with a pEGFP-LC3-expressing cDNA plasmid with either a control siRNA (siScrambled) or a siRNA directed against MT1-MMP (siMT1-MMP) as described in the section 2. Cells were then serum-starved in the presence or not of 10  $\mu$ M ARP101. Cells were fixed 24 hr later and the nuclei (blue) counterstained with Hoechst 33342. (a) Two representative pictures are shown for each condition. Even intracellular distribution of exogenous LC3 (green) suggests no autophagy is induced, whereas a more characteristic LC3 punctates formation suggests autophagy is induced. (b) LC3 punctates were quantified over untreated control by scanning densitometry. Representative pictures are shown from four independent experiments for each condition [Colour figure can be viewed at [wileyonlinelibrary.com](http://wileyonlinelibrary.com)]

10  $\mu$ M ARP101 for 24 hr, total RNA isolated, cDNA synthesized and qPCR performed as described in the section 2. The expression levels were then reported to untreated basal control conditions for each gene, respectively. We observed that ATG3 and ATG16 transcript levels were slightly, but not statistically significant, induced by ARP101, whereas ATG9 gene expression was significantly induced (Figure 7a). When MT1-MMP gene expression was transiently silenced (Figure 7b), we found that ARP101-induced ATG9 expression was abolished (Figure 7c). Collectively, these results suggest that ARP101 abrogates important intracellular MT1-MMP relays that control autophagy processes.

## 4 | DISCUSSION

In the current study, we investigated the dual pharmacological property of ARP101 in the combined targeting of MMP

catalytic functions and autophagy signaling functions (summarized in Figure 8). Such functions, which are molecularly associated to one crucial cell surface biomarker MT1-MMP, have both been found efficiently inhibited as assessed in a human grade IV glioblastoma cell model. We showed that ARP101 inhibited ConA-mediated proMMP-2 activation and MT1-MMP auto-proteolytic activity. When recombinant MT1-MMP was constitutively overexpressed, ARP101 again inhibited MT1-MMP-mediated proMMP-2 activation and auto-proteolytic functions, which, in part, correlated with the appearance of MT1-MMP oligomers and appeared to require MT1-MMP location at the plasma membrane. Finally, we show that ARP101 triggered autophagy as reflected through increased intracellular acidic vesicular organelle formation, increased LC3 punctate, and selective increase in ATG9 expression. Interestingly, all these autophagy-induced events were repressed when MT1-MMP was silenced confirming that ARP101 exerts some of its effects through MT1-MMP-mediated intracellular signaling

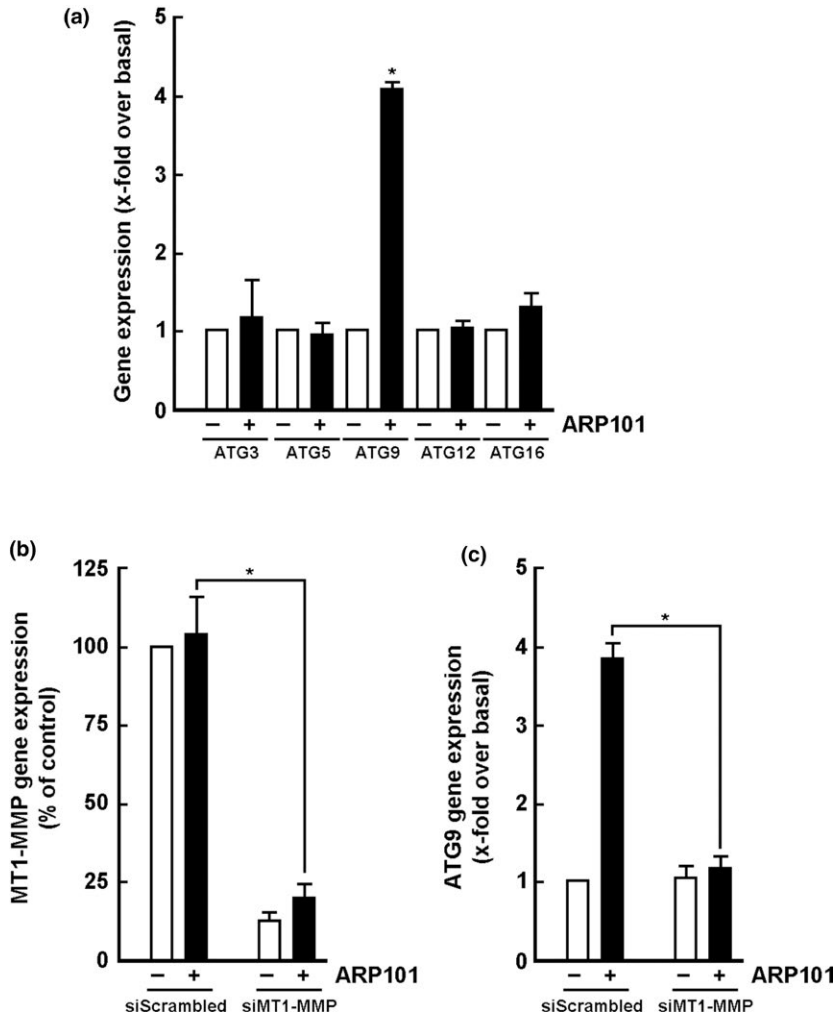


**FIGURE 7** ARP101 induces ATG9 autophagy biomarker gene expression and requires membrane type-1 matrix metalloproteinase (MT1-MMP) intracellular transducing functions. Serum-starved U87 glioblastoma cells were treated with or without 10  $\mu$ M ARP101 for 24 hr. (a) Total RNA was isolated, cDNA synthesized, and qPCR performed as described in the section 2 to assess ATG3, ATG5, ATG9, ATG12, and ATG16 transcript levels. (b) Serum-starved U87 glioblastoma cells were transiently transfected with a control siRNA (siScrambled) or a siRNA directed against MT1-MMP (siMT1-MMP); then, the cells were treated with or without ARP101, and (b) MT1-MMP or (c) ATG9 gene expression was assessed

that regulates autophagy. This represents the first molecular evidence supporting ARP101 dual targeting of a glioblastoma-associated biomarker functions in ECM degradation and cell invasion, as well as in the homeostatic balance of cell death/survival events involving autophagy.

Mechanistically, the current study also reveals the possible impact that MT1-MMP oligomerization states may have upon both the hydrolytic and signal-transducing functions of MT1-MMP leading to autophagy. While the MT1-MMP's ECM hydrolysis functions are well-documented,<sup>[42]</sup> its signal-transducing functions have only very recently been recognized. These signaling functions are mostly conferred through its cytoplasmic domain and have been found crucial in activating numerous intracellular pathways regulating autophagy,<sup>[24,43]</sup> inflammation,<sup>[44]</sup> endoplasmic reticulum stress,<sup>[29]</sup> and cell/death<sup>[28]</sup> processes. Among these pathways, MT1-MMP has further been found to relay signals that trigger the phosphorylation of intermediates such as JAK/STAT,<sup>[43]</sup> NF- $\kappa$ B,<sup>[45]</sup> Src,<sup>[46]</sup> and Erk<sup>[47]</sup> and to modulate RhoA/ROCK expression.<sup>[48]</sup> MT1-MMP's involvement in autophagy has also been reflected through the induction of autophagy biomarker Bcl-2/adenovirus E1B 19 kDa interacting protein 3

in glioblastoma cells,<sup>[43]</sup> and an upregulation of autophagy-related gene members ATG3, ATG12, and ATG16-like 1.<sup>[24]</sup> Whether the oligomerization states of MT1-MMP modulate any of these signaling pathways and how they impact on autophagy signaling remains to be better understood. ARP101 was demonstrated to inhibit both the MT1-MMP hydrolytic activity involved in auto-proteolysis, proMMP-2 activation, and the intracellular MT1-MMP-mediated signaling. Which domains of MT1-MMP are directly targeted by ARP101 still remains unclear although the catalytic domain is the first speculative option. Among the approaches that will be required to assess the targeting of MT1-MMP catalytic function, assays will need to be performed in vitro on recombinant soluble MT1-MMP catalytic forms.

The formation of multimeric MT1-MMP complexes is believed to facilitate its autocatalytic inactivation upon proMMP-2 activation at the cell surface.<sup>[37]</sup> Mutational analysis of MT1-MMP have revealed a role of the cytoplasmic tail Cys(574), the active site Glu(240), and furin cleavage motifs in oligomerization, processing, and auto-proteolysis of MT1-MMP in breast carcinoma cells.<sup>[49]</sup> Given MT-MMP activities appear to be spatially and timely regulated at multiple

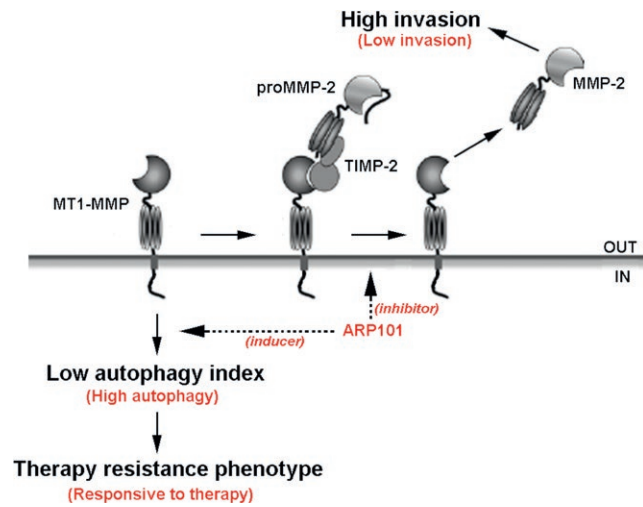


**FIGURE 8** Summarized scheme of ARP101 cellular effects on extracellular membrane type-1 matrix metalloproteinase (MT1-MMP)-mediated proMMP-2 activation and intracellular MT1-MMP-mediated signaling in brain cancer cells. ARP101 has both extracellular effects and intracellular effects targeting MT1-MMP-mediated functions. A human glioblastoma-derived grade IV (U87 glioblastoma) cell model has been used in this study to reflect the low autophagy index of high-grade gliomas.<sup>[9]</sup> MT1-MMP-mediated proMMP-2 activation into MMP-2 has been observed upon concanavalin-A treatment and confirmed as assessed by zymography. Such event is classically known to correlate with a high invasion phenotype. Involvement of MT1-MMP-mediated signaling in autophagy has also been known to require its intracellular domain and is believed to correlate with some therapy resistance phenotype. ARP101 effects are denoted in red. Whereas it inhibited MT1-MMP-mediated proMMP-2 activation ultimately leading to decreased invasion, ARP101 exploited MT1-MMP-mediated signaling to trigger autophagy and eventually allow for some therapy response [Colour figure can be viewed at [wileyonlinelibrary.com](http://wileyonlinelibrary.com)]

levels by microtubular vesicular trafficking,<sup>[29]</sup> MT1-MMP's oligomerization interactions and localization in the actin-based invadosomes may further regulate the infiltrating phenotype of glioblastoma cells.<sup>[26]</sup> In this study, we demonstrate that proper trafficking of MT1-MMP from intracellular compartment to the cell surface allows for ARP101-mediated oligomerization to occur. Indeed, when vesicular trafficking of MT1-MMP was altered upon Brefeldin-A treatment, ARP101 was unable to trigger MT1-MMP oligomerization suggesting that ARP101 possibly required MT1-MMP to be located at the plasma membrane in order to exert its autophagy inducing effects. MT1-MMP immunophenotyping was performed by flow cytometry in order to assess whether ARP101 treatment altered cell surface MT1-MMP expression. We found no differences between control and ARP101 treatment (not shown). Interestingly, the cell surface localization of MT1-MMP, rather than its proteolytic processing, was found to contribute to the ER stress induction process.<sup>[29]</sup> In support, ER stress-induced autophagy and apoptosis in cervical tumor cells was recently reported.<sup>[50]</sup> Intriguingly, the

biological significance of the transient ARP101-mediated formation of MT1-MMP dimers followed by the formation of MT1-MMP tetramers at higher ARP101 concentrations remains unknown. While these MT1-MMP tetramers correlate with reduced proMMP-2 activation and increased autophagy as reflected by increased LC3 puncta and ATG9 expression, further investigations are, however, required. ATG9 being the only transmembrane protein in the autophagy core machinery to play a key role in directing membrane from donor organelles for autophagosome formation,<sup>[51,52]</sup> it also remains to be understood how ARP101-mediated increase in ATG9 transcription occurs. Lastly, given MT1-MMP is characterized by a transmembrane domain and the presence of an insertion of 11 amino-acids between its pro-peptide and its catalytic domain, which may be cleaved by Furin-like enzymes leading to the maturation and activation of MT1-MMP forms,<sup>[53]</sup> one can also hypothesize that ARP101 concomitantly targets such Furin activity as well.

Over the last decade, pharmacological progress toward glioblastoma patient treatment remained challenging. Among the numerous molecular and cellular phenotype of brain tumors, low patient survival rate was correlated with the acquisition of their adaptive and invasive phenotype<sup>[54]</sup> as well as the development of a chemoresistant phenotype in part attributable to autophagy.<sup>[38]</sup> Whereas high expression of MT1-MMP in brain tumors strongly contributed to the infiltrating nature of this type of tumor,<sup>[55]</sup> design of an optimal pharmacological inhibition strategy of MT1-MMP, such as through ARP101, may eventually be envisioned in future therapy modalities against brain cancer.

## ACKNOWLEDGMENTS

This work was funded by the Institutional Research Chair in Cancer Prevention and Treatment held by Dr Borhane Annabi at UQAM.

## CONFLICT OF INTEREST

The authors declare no potential conflict of interests with respect to the research, authorship, and/or publication of this article.

## AUTHOR CONTRIBUTION

MD performed all the experiments, analyzed the data, and drafted the manuscript. BA designed the study, analyzed the data, and drafted the manuscript. All authors read and approved the final manuscript.

## ORCID

Borhane Annabi  <http://orcid.org/0000-0002-5082-7183>

## REFERENCES

- [1] S. Osuka, E. G. Van Meir, *J. Clin. Invest.* **2017**, *127*(2), 415.
- [2] J. J. Miller, P. Y. Wen, *Expert Opin. Emerg. Drugs* **2016**, *21*, 441.
- [3] A. K. Abdel-Aziz, A. B. Abdel-Naim, S. Shouman, S. Minucci, M. Elgendy, *Front. Pharmacol.* **2017**, *8*, 718.
- [4] Y. Lei, D. Zhang, J. Yu, H. Dong, J. Zhang, S. Yang, *Cancer Lett.* **2017**, *393*, 33.
- [5] L. Liu, J. Z. Liao, X. X. He, P. Y. Li, *Oncotarget* **2017**, *8*, 57707.
- [6] H. G. Wirsching, E. Galanis, M. Weller, *Handb. Clin. Neurol.* **2016**, *134*, 381.
- [7] S. Jawhari, M. H. Ratinaud, M. Verdier, *Cell Death Dis.* **2016**, *7*, e2434.
- [8] J. Noonan, J. Zarrer, B. M. Murphy, *Crit. Rev. Oncog.* **2016**, *21*, 241.
- [9] X. Huang, H. M. Bai, L. Chen, B. Li, Y. C. Lu, *J. Clin. Neurosci.* **2010**, *17*, 1515.
- [10] D. Kögel, S. Fulda, M. Mittelbronn, *Anticancer Agents Med. Chem.* **2010**, *10*, 438.
- [11] S. Hombach-Klonisch, M. Mehrpour, S. Shojaei, C. Harlos, M. Pitz, A. Hamai, K. Siemianowicz, W. Likus, E. Wiechec, B. D. Toyota, R. Hoshyar, A. Seyfoori, Z. Sepehri, S. R. Ande, F. Khadem, M. Akbari, A. M. Gorman, A. Samali, T. Klonisch, S. Ghavami, *Pharmacol. Ther.* **2018**, *184*, 31.
- [12] R. Pinheiro, C. Braga, G. Santos, M. R. Bronze, M. J. Perry, R. Moreira, D. Brites, A. S. Falcão, *ACS Chem. Neurosci.* **2017**, *8*, 50.
- [13] L. Zhang, H. D. Wang, X. J. Ji, Z. X. Cong, J. H. Zhu, Y. Zhou, *Oncol. Rep.* **2013**, *30*, 2571.
- [14] A. Estrada-Bernal, K. Palanichamy, A. Ray Chaudhury, J. R. Van Brocklyn, *Neuro. Oncol.* **2012**, *14*(4), 405.
- [15] L. Zhang, H. Wang, K. Ding, J. Xu, *Toxicol. Lett.* **2015**, *236*, 43.
- [16] L. Zhang, H. Wang, *Pharmacol. Rep.* **2017**, *69*, 1186.
- [17] S. He, Q. Li, X. Jiang, X. Lu, F. Feng, W. Qu, Y. Chen, H. Sun, *J. Med. Chem.* **2018**, *61*, 4656.
- [18] Y. K. Jo, S. J. Park, J. H. Shin, Y. Kim, J. J. Hwang, D. H. Cho, J. C. Kim, *Biochem. Biophys. Res. Commun.* **2011**, *404*, 1039.
- [19] E. I. Deryugina, B. Ratnikov, E. Monosov, T. I. Postnova, R. DiScipio, J. W. Smith, A. Y. Strongin, *Exp. Cell Res.* **2001**, *263*, 209.
- [20] H. D. Foda, S. Zucker, *Drug Discov. Today* **2001**, *6*, 478.
- [21] Y. Itoh, *Matrix Biol.* **2015**, *44–46*, 207.
- [22] J. H. Chang, Y. H. Huang, C. M. Cunningham, K. Y. Han, M. Chang, M. Seiki, Z. Zhou, D. T. Azar, *Surv. Ophthalmol.* **2016**, *61*, 478.
- [23] H. Mori, R. Bhat, A. Bruni-Cardoso, E. I. Chen, D. M. Jorgens, K. Coutinho, K. Louie, B. B. Bowen, J. L. Inman, V. Tecca, S. J. Lee, S. Becker-Weimann, T. Northen, M. Seiki, A. D. Borowsky, M. Auer, M. J. Bissell, *PeerJ* **2016**, *4*, e2142.
- [24] J. Pratt, R. Roy, B. Annabi, *Glycobiology* **2012**, *22*, 1245.
- [25] S. Sheehy, B. Annabi, *Gene Regul. Syst. Bio.* **2017**, *11*, 1177625017713996.
- [26] S. P. Turunen, O. Tatti-Bugaeva, K. Lehti, **2017**. *Biochim. Biophys. Acta.* *1864*(11 Pt A), 1974
- [27] R. Shimizu-Hirota, W. Xiong, B. T. Baxter, S. L. Kunkel, I. Maillard, X. W. Chen, F. Sabeh, R. Liu, X. Y. Li, S. J. Weiss, *Genes Dev.* **2012**, *26*, 395.
- [28] A. Belkaid, S. Fortier, J. Cao, B. Annabi, *Neoplasia* **2007**, *9*, 332.
- [29] S. Proulx-Bonneau, J. Pratt, B. Annabi, *J. Neurooncol.* **2011**, *104*(1), 33.
- [30] P. K. Panda, S. Mukhopadhyay, D. N. Das, N. Sinha, P. P. Naik, S. K. Bhutia, *Semin. Cell Dev. Biol.* **2015**, *39*, 43.
- [31] C. P. Kung, A. Budina, G. Balaburski, M. K. Bergenstock, M. Murphy, *Crit. Rev. Eukaryot. Gene Expr.* **2011**, *21*, 71.
- [32] S. J. Atkinson, C. Roghi, G. Murphy, *Biochem. J.* **2006**, *398*, 15.
- [33] J. A. Cho, P. Osenkowski, H. Zhao, S. Kim, M. Toth, K. Cole, A. Aboukameel, A. Saliganan, L. Schuger, R. D. Bonfil, R. Fridman, *J. Biol. Chem.* **2008**, *283*, 17391.
- [34] S. Ingvarsen, D. H. Madsen, T. Hillig, L. R. Lund, K. Holmbeck, N. Behrendt, L. H. Engelholm, *Biol. Chem.* **2008**, *389*, 943.
- [35] K. Lehti, J. Lohi, H. Valtanen, J. Keski-Oja, *Biochem. J.* **1998**, *334*(Pt 2), 345.
- [36] Y. Itoh, N. Ito, H. Nagase, R. D. Evans, S. A. Bird, M. Seiki, *Mol. Biol. Cell* **2006**, *17*(12), 5390.
- [37] K. Lehti, J. Lohi, M. M. Juntunen, D. Pei, J. Keski-Oja, *J. Biol. Chem.* **2002**, *277*, 8440.
- [38] J. Pratt, M. Iddir, S. Bourgault, B. Annabi, *Mol. Carcinog.* **2016**, *55*, 148.
- [39] A. Sina, S. Proulx-Bonneau, A. Roy, L. Poliquin, J. Cao, B. Annabi, *J. Cell. Commun. Signal.* **2010**, *4*, 31.
- [40] R. D. Klausner, J. G. Donaldson, J. Lippincott-Schwartz, *J. Cell Biol.* **1992**, *116*(5), 1071.
- [41] H. R. Pugsley, *Methods* **2017**, *112*, 147.
- [42] W. Hornebeck, H. Emonard, J. C. Monboisse, G. Bellon, *Semin. Cancer Biol.* **2002**, *12*(3), 231.
- [43] J. Pratt, B. Annabi, *Cell. Signal.* **2014**, *26*, 917.
- [44] N. Akla, J. Pratt, B. Annabi, *Exp. Cell Res.* **2012**, *318*, 2498.
- [45] B. Annabi, C. Laflamme, A. Sina, M. P. Lachambre, R. Béliveau, *J. Neuroinflammation* **2009**, *6*, 8.
- [46] A. Zgheib, S. Lamy, B. Annabi, *J. Biol. Chem.* **2013**, *288*, 13378.
- [47] D. Gingras, N. Bousquet-Gagnon, S. Langlois, M. P. Lachambre, B. Annabi, R. Béliveau, *FEBS Lett.* **2001**, *507*, 231.
- [48] B. Annabi, M. Bouzegrane, R. Moumdjian, A. Moghrabi, R. Béliveau, *J. Neurochem.* **2005**, *94*, 906.
- [49] D. V. Rozanov, E. I. Deryugina, B. I. Ratnikov, E. Z. Monosov, G. N. Marchenko, J. P. Quigley, A. Y. Strongin, *J. Biol. Chem.* **2001**, *276*, 25705.
- [50] X. Zhu, L. Huang, J. Gong, C. Shi, Z. Wang, B. Ye, A. Xuan, X. He, D. Long, X. Zhu, N. Ma, S. Leng, *Cell Death Discov.* **2017**, *3*, 17059.
- [51] Y. Feng, D. J. Klionsky, *Cell Res.* **2017**, *27*, 161.
- [52] X. Zhuang, K. P. Chung, Y. Cui, W. Lin, C. Gao, B. H. Kang, L. Jiang, *Proc. Natl Acad. Sci. USA* **2017**, *114*(3), E426.
- [53] M. Polette, P. Birembaut, *Int. J. Biochem. Cell Biol.* **1998**, *30*, 1195.
- [54] S. Mehta, C. Lo Cascio, *Cell. Mol. Life Sci.* **2018**, *75*, 385.
- [55] D. S. Markovic, K. Vinnakota, S. Chirasani, M. Synowitz, H. Raguette, K. Stock, M. Sliwa, S. Lehmann, R. Kälin, N. van Rooijen, K. Holmbeck, F. L. Heppner, J. Kiwit, V. Matyash, S. Lehnardt, B. Kaminska, R. Glass, H. Kettenmann, *Proc. Natl Acad. Sci. USA* **2009**, *106*(30), 12530.

**How to cite this article:** Desjarlais M, Annabi B. Dual functions of ARP101 in targeting membrane type-1 matrix metalloproteinase: Impact on U87 glioblastoma cell invasion and autophagy signaling. *Chem Biol Drug Des.* 2019;93:272–282. <https://doi.org/10.1111/cbdd.13410>